Key Points:
- It takes ~50 Myr to form degree-2 mantle structure in all the plate motion models
- The degree-2 structure may have been formed by 200 Ma the latest
- No published plate motion models predict stationary Africa and Pacific LLSVPs

Correspondence to:
S. Zhong,
szhong@colorado.edu

On the temporal evolution of long-wavelength mantle structure of the Earth since the early Paleozoic

Shijie Zhong[1] and Maxwell L. Rudolph[2]

[1]Department of Physics, University of Colorado, Boulder, Colorado, USA, [2]Department of Geology, Portland State University, Portland, Oregon, USA

Abstract The seismic structure of the Earth's lower mantle is characterized by a dominantly degree-2 pattern with the African and Pacific large low shear velocity provinces (i.e., LLSVP) that are separated by circum-Pacific seismically fast anomalies. It is important to understand the origin of such a degree-2 mantle structure and its temporal evolution. In this study, we investigated the effects of plate motion history and mantle viscosity on the temporal evolution of the lower mantle structure since the early Paleozoic by formulating 3-D spherical shell models of thermochemical convection. For convection models with realistic mantle viscosity and no initial structure, it takes about ~50 Myr to develop dominantly degree-2 lower mantle structure using the published plate motion models for the last either 120 Ma or 250 Ma. However, it takes longer time to develop the mantle structure for more viscous mantle. While the circum-Pangea subduction in plate motion history models promotes the formation of degree-2 mantle structure, the published pre-Pangea plate motions before 330 Ma produce relatively cold lower mantle in the African hemisphere and significant degree-1 structure in the early Pangea (~300 Ma) or later times, even if the lower mantle has an initially degree-2 structure and a viscosity as high as 10^{23} Pas. This suggests that the African LLSVP may not be stationary since the early Paleozoic. With the published plate motion models and lower mantle viscosity of 10^{22} Pas, our mantle convection models suggest that the present-day degree-2 mantle structure may have largely been formed by ~200 Ma.

1. Introduction

Global seismic imaging of the Earth's mantle [*Dziewonski*, 1984; *Woodhouse and Dziewonski*, 1984; *Tanimoto*, 1990; *Grand et al.*, 1997; *Becker and Boschi*, 2002; *Panning and Romanowicz*, 2006; *Ritsema et al.*, 2011] has profoundly shaped our understanding of the Earth's dynamics. The seismic models demonstrate that the Earth's lower mantle is characterized by two major seismically slow anomalies below Africa and Pacific that are surrounded by circum-Pacific seismically fast anomalies, i.e., a spherical harmonic degree-2 structure [e.g., *Tanimoto*, 1990; *Ritsema et al.*, 2011]. The two major seismically slow anomalies below Africa and Pacific are sometimes also referred to as large low shear velocity provinces (i.e., LLSVPs). Recent seismic studies suggest that the LLSVPs may be chemically distinct from the overlying mantle [e.g., *Masters et al.*, 2000; *Wen et al.*, 2001; *Ni et al.*, 2002; *Simmons et al.*, 2010], although the volume of the chemically distinct LLSVPs may only account for several percent of the mantle [*Houser et al.*, 2008; *He and Wen*, 2012]. The seismic structure of the lower mantle has made it possible to integrate and understand a variety of observations including plate tectonics, long-wavelength gravity and topography anomalies, hotspot volcanism, and mantle geochemical anomalies. It has also posed challenging questions on the origin and dynamics of such long-wavelength mantle structure.

It was recognized in the early seismic tomography studies that the circum-Pacific seismically fast anomalies in the lower mantle were closely associated with subduction zones [*Dziewonski*, 1984; *Su et al.*, 1994; *Tanimoto*, 1990]. Global mantle flow models show that plate motions have important controls on mantle flow patterns such that beneath surface plate convergence (divergence) are mantle downwelling (upwelling) flows [e.g., *Hager and O'Connell*, 1979]. Time-dependent convection models with a uniform composition (i.e., isochemical or purely thermal models of mantle convection) using plate motion history for the last 120 Myr as time-dependent boundary conditions [e.g., *Lithgow-Bertelloni and Richards*, 1998] reproduced well the circum-Pacific seismically fast structure as subducted slabs, although they had only limited success in explaining the large-scale seismically slow structures (i.e., LLSVPs) [e.g., *Bunge et al.*, 2002]. However,

including chemically dense materials with volume similar to that inferred seismically for the LLSVPs [*He and Wen*, 2012; *Houser et al.*, 2008], thermochemical mantle convection models reproduced both the African and Pacific LLSVPs and the circum-Pacific downwelling structures [*McNamara and Zhong*, 2005; *Bull et al.*, 2009; *Zhang et al.*, 2010; *Bower et al.*, 2012]. However, recent isochemical convection models showed an improved fit to the LLSVP structures, suggesting that the LLSVPs may be interpreted as purely thermal origins without chemical heterogeneities [e.g., *Davies et al.*, 2012; *Schuberth et al.*, 2009]. These convection models demonstrated that the present-day long-wavelength mantle structure as revealed from seismic studies is controlled by plate motion history in the last 100–150 Myr [*Bunge et al.*, 1998; *McNamara and Zhong*, 2005].

While the seismic structure represents a snapshot of the present-day's mantle, recent studies have also started to explore time evolution of mantle structure in Earth's geological history [e.g., *Torsvik et al.*, 2010; *Zhong et al.*, 2007]. *Torsvik et al.* [2010, 2014] proposed that the mantle may have had a predominantly degree-2 structure that is similar to the present-day's mantle with African and Pacific LLSVPs for the last 500 Ma. This proposal was largely based on spatial correlation of eruption sites of large igneous provinces (LIP) and kimberlites with the edges of LLSVPs [*Torsvik et al.*, 2006, 2010]. Previously, hotspot volcanism was found to preferentially locate in the African and Pacific LLSVPs [*Hager et al.*, 1985] or in the regions with the largest horizontal gradients in S wave velocity models [*Thorne et al.*, 2004]. Using the stationary African and Pacific LLSVPs as a reference frame for the last 500 Ma and the assumption that LIPs and kimberlites would always erupt at the edges of LLSVPs, *Torsvik et al.* [2014] and *Domeier and Torsvik* [2014] have reconstructed paleogeography of continents, global plate motions, and true polar wander events for the Paleozoic.

An alternative proposal, on the basis of geodynamic arguments, is that the mantle had a predominantly degree-1 structure in the Paleozoic lasting through the early stages of Pangea assembly, and that the African LLSVP did not form until ∼200–300 Ma [*Zhong et al.*, 2007; *Li and Zhong*, 2009]. The proposed time evolution of mantle structure since the Paleozoic is consistent with thermochemical mantle convection models with a plate motion history model for the last 450 Ma that considers the assembly and breakup of Pangea [*Zhang et al.*, 2010; *Rudolph and Zhong*, 2014]. The plate motion history used in these convection models combines plate motions for the last 120 Ma from *Lithgow-Bertelloni and Richards* [1998] and that derived from paleogeography by *Scotese* [2001]. The significant convergence between Laurussia and Gondwana from 450 to 330 Ma in *Scotese*'s paleogeography model leads to accumulation of cold, subducted slabs beneath Pangea, clearing the thermochemical materials from the African/Pangea hemisphere that does not start to form the African LLSVP until ∼200 Ma [*Zhang et al.*, 2010]. The mantle convection models also predict time-dependent surface dynamic topography and core mantle boundary (CMB) heat flux that have been used in interpreting vertical motion history of continental cratons [*Zhang et al.*, 2012; *Flowers et al.*, 2012] and polarity reversals of geomagnetic field [*Olson et al.*, 2013, 2015; *Zhang and Zhong*, 2011].

Recently, *Bull et al.* [2014] performed thermochemical convection calculations using the Paleozoic (410–250 Ma) plate motion by *Domeier and Torsvik* [2014] and the plate motions for the last 200 Ma by *Seton et al.* [2012], and stated that their results differed significantly from that reported in *McNamara and Zhong* [2005] and *Zhang et al.* [2010]. *Bull et al.* [2014] concluded that the African and Pacific LLSVPs would have remained close to their present-day positions for at least the last 410 Myr, supporting *Torsvik et al.* [2010, 2014]. Their study also suggested that mantle structure could not have been dominantly degree-1 during Pangea assembly, and that the present-day degree-2 mantle structure with two LLSVPs would require much longer plate motion history than the last 120 Myr to generate, as suggested previously by *Bunge et al.* [1998] and *McNamara and Zhong* [2005].

The goal of our study is to further explore the controls on mantle structures including the effects of plate motions and mantle viscosity. We are particularly interested in examining when the present-day degree-2 mantle structure with the African and Pacific LLSVPs is generated and how stationary this structure is back in time, using different plate motion models [*Domeier and Torsvik*, 2014; *Seton et al.*, 2012; *Zhang et al.*, 2010; *Lithgow-Bertelloni and Richards*, 1998]. *Rudolph and Zhong* [2014] examined the effect of plate motion history by *Seton et al.* [2012] on the mantle structure relative to that from *Zhang et al.* [2010], and did not find significant difference from those two plate motion models. However, *Rudolph and Zhong* [2014] only presented one case for comparison of the mantle structure, as it was not the main focus of that study. In this study, we will systematically explore the effects of different convection model parameters and plate motion models. The paper is organized as follows: Section 2 describes the thermochemical convection

Table 1. Physical and Model Parameters

Parameters	Value
Earth's radius	6370 km
Core-mantle boundary radius	3503 km
Mantle density	3300 kg/m^3
Coefficient of thermal expansion	3×10^{-5}/K
Thermal diffusivity	10^{-6} m^2/s
Gravitational acceleration	9.8 m/s^2
Temperature across the mantle	2500 K

model and plate motion history model. Section 3 is for the results, and discussion and conclusions are given in sections 4 and 5, respectively.

2. Models for Mantle Convection and History of Plate Motions

2.1. Convection Models

This study employs semidynamic models of mantle convection in a three-dimensional spherical geometry, using time-dependent plate motions as surface boundary conditions and assuming an infinite Prandtl number and the Boussinesq approximation. The models consider a chemically distinct layer with a larger density above the CMB. The models are the same as *McNamara and Zhong* [2005] and *Zhang et al.* [2010], except for using different plate motions, viscosity, and chemical density. The models including governing equations are fully described in *Zhang et al.* [2010], and here we only briefly describe the models.

The surface and CMB are at nondimensional radius 1 and 0.55, respectively. Isothermal boundary conditions are applied at the surface and CMB in all calculations. The surface is prescribed with time-dependent velocity (i.e., plate motion), while the CMB is with free-slip boundary condition. Unless specified otherwise, most cases start with an initially flat 250 km thick chemical layer above the CMB, leading to a volume of the chemically distinct material that is comparable with the seismic observations [e.g., *Houser et al.*, 2008; *He and Wen*, 2012]. Most cases also start with an 1-D initial temperature profile derived from a precalculation that uses similar model parameters except that the plate motion boundary condition is replaced with free-slip boundary conditions [e.g., *McNamara and Zhong*, 2005].

There are four model parameters: thermal Rayleigh number Ra, buoyancy number B, internal heat generation rate H, and mantle rheology [*Zhang et al.*, 2010]. The relevant physical and model parameters are listed in Tables 1 and 2. Ra controls convective vigor of thermal convection, and is chosen to be broadly consistent with the imposed plate motion. H is chosen to yield ~50% internal heating rate. The buoyancy number B defines the behavior of the chemically dense layer above the CMB. The larger B is, the less entrainment mantle convection can cause to the chemical layer, and the smaller topography for the chemical interface is [e.g., *Tackley*, 1998]. The nondimensional depth and temperature-dependent viscosity is

$$\eta(T, r) = \eta_0(r) \exp\left[E(0.5 - T)\right], \tag{1}$$

where $\eta_0(r)$ is the depth-dependent prefactor and E is the activation energy nondimensionalized by $R\Delta T$, where R is the gas constant and ΔT is the temperature across the mantle. Nondimensional activation energy E is 9.21, leading to temperature-induced viscosity variations of 10^4. The relatively small activation energy is used here for numerical stability and also to account for other weakening effects such as brittle deformation

Table 2. Model Parameters and Initial and Boundary Conditions

Case	Start Time (Ma)	Plate Motion[a]	Ra	B	Initial Condition[b]
1	120	S	2×10^8	0.5	1-D
2	120	LBR	2×10^8	0.5	1-D
3	250	DT + S	2×10^8	0.5	1-D
4	250	Z + LBR	2×10^8	0.5	1-D
5	410	DT + S	2×10^8	0.5	1-D
6	458	Z + LBR	2×10^8	0.5	1-D
7	250	DT + S	7×10^7	0.6	1-D
8	250	DT + S	2×10^7	0.7	1-D
9	410	DT + S	2×10^8	0.5	Case 5
10	410	DT + S	2×10^8	0.5	Case 4
11	410	DT + S	7×10^7	0.6	Case 7
12	410	DT + S	2×10^7	0.7	Case 8

[a]Among different plate motion history models, S, LBR, DT, and Z represent *Seton et al.* [2012], *Lithgow-Bertelloni and Richards* [1998], *Domeier and Torsvik* [2014], and *Zhang et al.* [2010], respectively.
[b]For initial condition, "1-D" represents using 1-D temperature and composition profiles with no lateral variations as initial conditions. "Case N" means that the present-day 3-D thermochemical structures from Case N are used as initial conditions, where N is case number (4 or 5).

and non-Newtonian rheology. The depth-dependent viscosity prefactor $\eta_0(r)$ is specified to give rise to a viscosity increase at the 670 km depth by a factor of 100 from the upper to lower mantle.

The models are computed with the code CitcomS [*Zhong et al.*, 2008] that was modified from an original Cartesian code [*Moresi et al.*, 1996; *Moresi and Solomatov*, 1995]. A particle-ratio method is used to solve the advection equation of composition and was incorporated to CitcomS by *McNamara and Zhong* [2004] [see *Zhong et al.*, 2008]. The mantle is divided into 12 blocks and each block can be divided in three directions for parallel computing [e.g., *Zhong et al.*, 2000, 2008]. The models are computed using a grid with 12×64^3 elements that should provide sufficient resolution for the results that are relevant to large-scale mantle structure [*Zhang et al.*, 2010].

2.2. Plate Motion History Models

The semidynamic mantle convection models use time-dependent plate motions as surface velocity boundary conditions. A number of different plate motions are considered here, and they cover different geological time periods and have different levels of robustness. In general, the further back in time, the poorer constrained the plate motions are, due to the lack of robust observations. The first plate motion model is from *Lithgow-Bertelloni and Richards* [1998, hereinafter referred to as LBR1998] for the last 119 Ma that combines previous work for the Cenozoic [*Gordon and Jurdy*, 1986] and for the late Mesozoic [*Engebretson et al.*, 1992; *Scotese*, 2001]. Figures 1a and 1b show plate motions at ∼100 Ma and present-day of this model. The second plate motion model is from *Zhang et al.* [2010, hereinafter referred to as Z2010] between 119 Ma and 450 Ma. Z2010 considered the Pangea assembly and breakup from a paleogeographic reconstruction [*Scotese*, 2001], while assuming that the Paleo-Pacific plate motions are similar to that in LBR1998 at 119 Ma. Figures 1c and 1d are for plate motions at ∼250 Ma and ∼380 Ma. Note that Pangea was assembled at ∼330 Ma and started to break up at ∼180 Ma [*Scotese*, 2001], and hence the plate motions at 250 Ma represent well plate motions during the Pangea time. The model calculations in *Zhang et al.* [2010] used plate motion models of Z2010 and LBR1998.

The third plate motion model is from *Seton et al.* [2012, hereinafter referred to as S2012] for the last 200 Ma. S2012 model represents an extension of plate motion model by *Müller et al.* [2008]. S2012 model shows similarity with plate motion models LBR1998 and Z2010 for continental plates, but for the Paleo-Pacific region, S2012 shows noticeable difference from LBR1998 before 80 Ma (Figure 1e). The last plate motion model is from *Domeier and Torsvik* [2014, hereinafter referred to as DT2014] for 410–250 Ma. This plate motion model was built based on the iterative scheme discussed in section 1 that assumed the fixity of African and Pacific LLSVPs for the last 500 Ma and accounted for true polar wander [*Torsvik et al.*, 2014]. The paleogeographic reconstruction associated with DT2014 differs significantly from that by *Scotese* [2001] before Pangea assembly, hence DT2014 and Z2010 plate motions are also different (Figure 1g). However, at 250 Ma during the Pangea time, DT2014 and Z2010 do not differ significantly (Figure 1f). *Bull et al.* [2014] used DT2014 and S2012 plate motions in similar semidynamic models of mantle convection.

The divergence of surface plate motions $\vec{V}$, $D = \nabla \cdot \vec{V}$, measures subduction and seafloor spreading plate motions and directly affects the mantle flow [e.g., *Hager and O'Connell*, 1981]. Degree-variance of divergence D_l can be defined by cosine and sine coefficients of spherical expansion of divergence D, C_{lm} and S_{lm}, as

$$D_l = \sqrt{\frac{1}{l(l+1)} \sum_{m=0}^{l} (C_{lm}^2 + S_{lm}^2)}, \qquad (2)$$

where l and m are the spherical harmonic degree and order. Note that the spherical harmonic expansion used here is defined in *Zhong et al.* [2008] as in CitcomS code. Long-wavelength degree-variances are relatively easy to be related to simple plate motion patterns. For example, degree-1 variance measures hemispherically asymmetric plate motion with plate divergence (i.e., seafloor spreading) in one hemisphere while plate convergence (i.e., subduction) in the other hemisphere. Degree-2 variance reflects two major seafloor spreading systems or two major subduction systems. The time-dependences of degree-variance of divergence of plate motions show significant time-variations for all the plate motion models (Figure 2). In general, for the last 120 Ma, S2012 and LBR1998 show similar time-dependence of divergence. Particularly, degree-variance decreases toward the present-day and degree-1 variance is stronger than degree-2. Between 120 and 200 Ma, degree-variances at degrees 1 and 2 are comparable in S2012, but degree-2 variance is larger than degree-1 variance in Z2010. Before Pangea assembly (i.e., before 330 Ma), degree-1
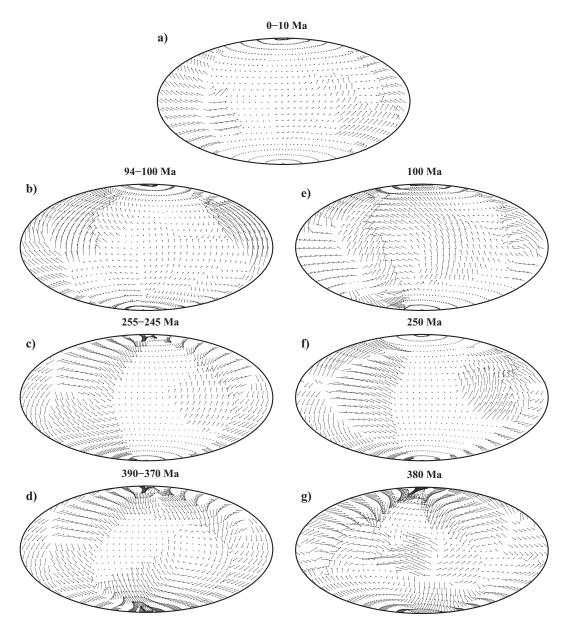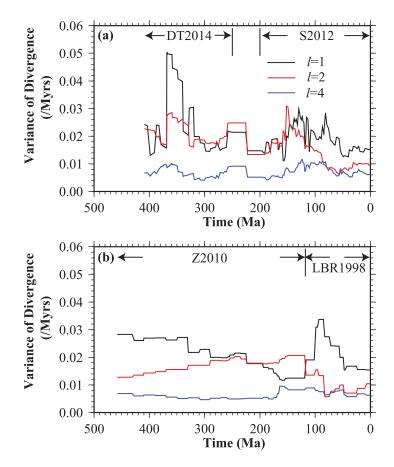
Figure 1. Plate motion models at different times. LBR1998 [*Lithgow-Bertelloni and Richards*, 1998] for the (a) present-day and (b) ∼100 Ma, Z2010 [*Zhang et al.*, 2010] at (c) ∼250 Ma and (d) ∼380 Ma, S2012 [*Seton et al.*, 2012] at (e) 100 Ma, and DT2014 [*Domeier and Torsvik*, 2014] at (f) 250 Ma and (g) 380 Ma.

variance is larger than that at degree-2 in Z2010, reflecting the overall convergent plate motion between Gondwana and Laurussia in the African hemisphere and divergent plate motion in the paleo-Pacific hemisphere (i.e., degree-1 flow pattern) [*Zhang et al.*, 2010]. However, when Pangea existed (i.e., between 330 Ma and 200 Ma), degree-1 and degree-2 variances are comparable in Z2010. For DT2014, degree-1 and degree-2 variances are comparable between 410 Ma and 250 Ma, except for a short period between 370 Ma and 340 Ma when the degree-1 variance is larger (Figure 2). It should be pointed out that in Figure 2a the plate motions between 250 and 225 Ma are taken from those at 250 Ma in DT2014, while the plate motions between 225 and 200 Ma are from those at 200 Ma in S2012.

3. Results

To examine the effects of different plate motion history models and convection model parameters on time evolution of mantle structures, and to better understand the differences between *Bull et al.* [2014] and

Figure 2. Degree-variance of divergence of plate motions at degrees-1, 2, and 4 for different plate motion history models: (a) DT2014 and S2012 and (b) Z2010 and LBR1998. See text for plate motions between 250 Ma and 200 Ma in Figure 2a. Degrees-1, 2, and 4 components are in black, red, and blue colors, respectively.

McNamara and Zhong [2005] and *Zhang et al.* [2010], new model calculations have been performed. We first present results with different plate motion history including plate motions with different time periods, and then examine the effects of convection model parameters and initial mantle structure.

3.1. Effects of Plate Motion History on the Lower Mantle Structure

Cases 1 and 2 are computed only for the last 120 Myr using plate motion models S2012 and LBR1998, respectively. Except for having a shorter model time, these two cases are identical to Case FS1 in *Zhang et al.* [2010] for initial 1-D temperature and composition fields, temperature and depth-dependent viscosity, buoyancy number (B = 0.5), and Rayleigh number (Ra = 2 $\times$ 10^8) (see *Zhang et al.* [2010] for model details and their Table 2 for model parameters) (Table 2). With Ra = 2 $\times$ 10^8 and other model parameters in Table 1, the lower mantle viscosity is approximately 10^{22} Pa·s and is ~100 times larger than the upper mantle viscosity (Figures 3a and 3b for radial temperature and viscosity profiles), consistent with that inferred from postglacial rebound studies [e.g., *Simons and Hager*, 1997; *Mitrovica and Forte*, 2004]. Case 1 would be same as Case 120_SS of *Bull et al.* [2014]. Case 2 is similar to the standard case in *McNamara and Zhong* [2005] except for having more realistic Ra. It should be noted that plate motions in S2012 and LBR1998 models are generally in a good agreement except for before 80 Ma in some regions of the Pacific plates (Figures 1b, 1d, and 2). Both Cases 1 and 2 start at 120 Ma with 1-D temperature and composition structures that do not have any lateral variations.

Degree-2 structures in the lower mantle similar to the present-day's have already emerged by ~80 Ma (i.e., ~40 Myr after the models start) for both cases (Figures 4b and 4d). In this study, we use thermochemical structures at 2750 km depth to represent the lower mantle structure unless indicated otherwise. Both cases also show similar mantle structures for the last 80 Myr including for the present-day with two thermochemical piles beneath Africa and Pacific (Figures 4a and 4c). The similar mantle structure and its time-dependence in these cases largely reflect the similarities between plate motions in S2012 and LBR1998 at least at long wavelengths (Figure 2). However, there are also noticeable differences in the lower mantle structure between Cases 1 and 2, for example, beneath South America and southeast Africa at ~80 Ma (Figures 4b and 4d). In Case 2, the degree-2 structure in the lower mantle is comparable with degree-3 before 70 Ma and becomes the dominant at 70 Ma. For Case 1, the degree-2 structure is the dominant for the last 90 Myr (Figures 5a and 5b). This may be caused by the larger degree-2 divergence of plate motions in S2012 before 80 Ma than in LBR1998 (Figure 2). Also, for either case, no significant structure develops in the CMB region for the first 20 Myr of the model calculations (Figures 5a and 5b).
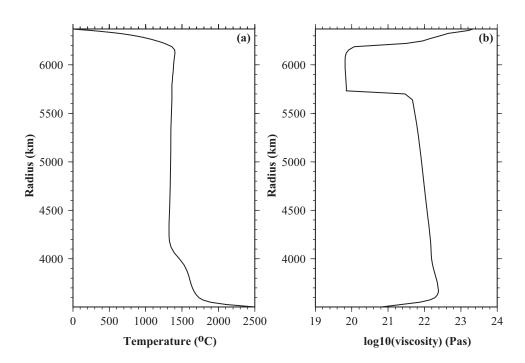
Figure 3. Horizontally averaged (a) temperature and (b) viscosity as a function of radius for Case 2 for the present-day. The dimensional results are from using parameters in Table 1. These temperature and viscosity profiles apply to all the cases except for Cases 7, 8, 11 and 12 that with their reduced Ra have an increased viscosity by a factor of 3 and 10, respectively, assuming that other parameters remain the same.
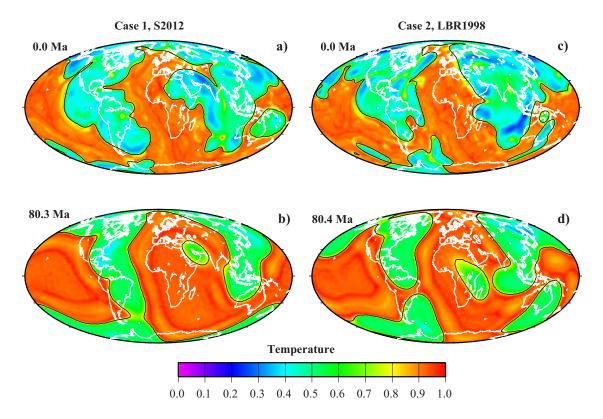

Figure 4. Snapshots of nondimensional temperature at 2750 km depth for Cases 1 and 2 that start at 120 Ma. For Case 1 with S2012 for the (a) present-day and (b) 80.3 Ma, and (c) for Case 2 with LBR1998 for the present-day and 80.4 Ma. For each figure, the black contour is for composition field C = 0.5 and chemical piles with C ∼ 1 are always significantly hotter than the ambient mantle. Coastlines are plotted in thin white lines.
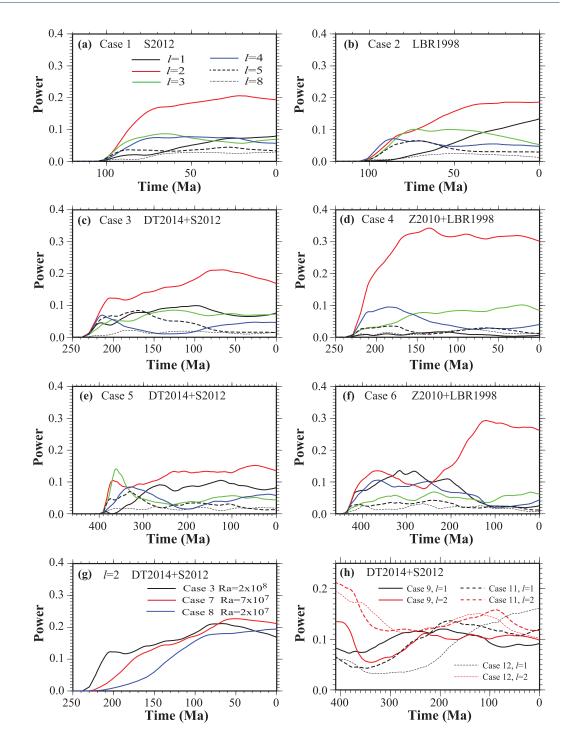
Figure 5. Time-dependence of degree power of the temperature structure at 2750 km depth for different spherical harmonic degrees *l* for Cases (a) 1, (b) 2, (c) 3, (d) 4, (e) 5, (f) 6, for degree-2 only for (g) Cases 3, 7, and 8, and for degree-1 and 2 for (h) Cases 9, 11, and 12. Note that the different time scales in the horizontal axes due to different times used for these cases.

The overall similarity of the lower mantle structure and its time evolution between Cases 1 and 2 suggests that the long-wavelength mantle structure is insensitive to the relatively small difference between S2012 and LBR1998 plate motions. This is consistent with *Rudolph and Zhong* [2014] that computed the models for the last 450 Myr with different plate motions only for the last 200 Myr. As expected, the present-day mantle structure from Case 2 (Figure 4c) is similar to *McNamara and Zhong* [2005], as they both use LBR1998 plate motion. However, Case 1 (Figure 4a) shows noticeably different present-day mantle structure
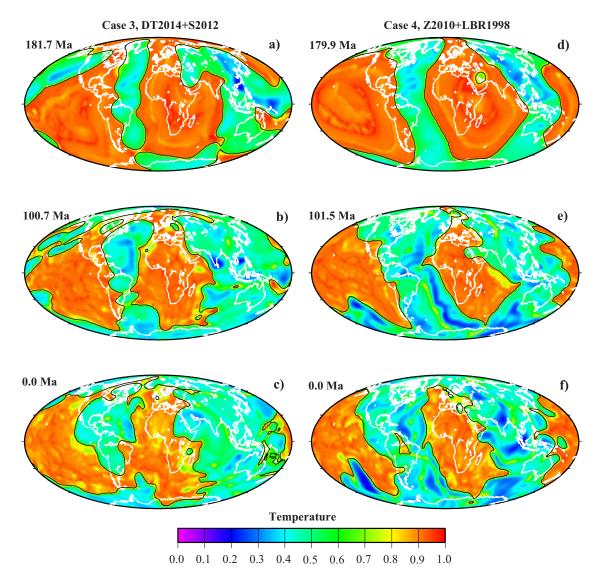
Figure 6. Snapshots of nondimensional temperature at 2750 km depth for Cases 3 and 4 that start at 250 Ma. For Case 3 with S2012/DT2014 at (a) ∼180 Ma, (b) ∼100 Ma and (c) for the present-day, and for Case 4 with LBR1998/Z2010 at (d) ∼180 Ma, (e) ∼100 Ma and (f) for the present-day. The black contour is for composition field C = 0.5.

from Case 120_SS of *Bull et al.* [2014] (e.g., under the western Pacific, Asia, and Indian Ocean), even though they both use S2012 plate motion.

Cases 3 and 4 are identical to Cases 1 and 2 except for using plate motion history for the last 250 Myr (Table 2). For Case 4, the plate motion is from LBR1998 for the last 120 Ma and is from *Zhang et al.* [2010] between 250 Ma and 120 Ma. For Case 3, plate motions for the last 200 Ma are taken from S2012, and plate motions at 250 Ma are from DT2014. Plate motions between 250 and 225 Ma are assumed to be those at 250 Ma from DT2014, while plate motions between 225 and 200 Ma are those at 200 Ma from S2012. The circum-Pangea subduction leads to significant degree-2 divergence in these plate motion models during the Pangea time including at and after 250 Ma (Figure 2). Both Cases 3 and 4 show strong degree-2 structures in the lower mantle by ∼200 Ma that are similar to the present-day with the African and Pacific chemical piles (Figures 6a and 6d at ∼180 Ma, and Figures 5c and 5d). The mantle structure in both cases is dominantly degree-2 and shows relatively small variations for the last 200 Myr even with the Pangea breakup (Figures 6b and 6c at ∼100 Ma and the present-day for Case 3, respectively, Figures 6e and 6f for Case 4, and Figures 5c and 5d). This is because the Pangea breakup does not significantly change the global subduction pattern that is the key to developing and maintaining the degree-2 mantle structure. This is also why an initially

degree-2 mantle structure that is similar to the present-day could be maintained largely unchanged in models that only use the plate motions for the last 250 Ma [*Bower et al.*, 2012]. Although Cases 3 and 4 show similar degree-2 structures, there are some interesting differences as well. For example, it appears that the two thermochemical piles in Case 3 with DT2014 and S2012 plate motions are closer to each other on the southeastern Pacific side than in Case 4 (Figures 6a–6c for Case 3). It also seems that Case 4 with LBR1998 and Z2010 plate motions reproduces the present-day degree-2 seismic structure better than Case 3. For example, the two chemical piles are separated in Case 4 (Figure 6f) as in the seismic models [e.g., *Ritsema et al.*, 2011], but they are connected beneath South America in Case 3 (Figure 6c).

Cases 5 and 6 use even longer plate motion history, but otherwise they are identical to Cases 1 and 2 (Table 2). Case 5 is computed using DT2014 and S2010 plate motion history for the last 410 Myr, while Case 6 is for the last 458 Myr using Z2010 and LBR1998. Case 6 is identical to Case FS1 of *Zhang et al.* [2010], except that Case 6 starts at 458 Ma with no initial "ramp-up" time period, unlike Case FS1 that included 150 Myr "ramp-up." Previously, *Zhang et al.* [2010] showed that in Z2010 plate motion model the plate convergence between Gondwana and Laurussia before 330 Ma would lead to a relatively cold lower mantle in the African hemisphere and hence degree-1 lower mantle structure in the early Pangea. On the other hand, *Bull et al.* [2014] reported that DT2014 plate motion history would stabilize the degree-2 lower mantle structure with the African and Pacific piles throughout the Paleozoic. Therefore, Cases 5 and 6 help to understand the time evolution of mantle structure during the Paleozoic.

In Case 5, the plate motion history in DT2014 leads to a rather complicated lower mantle structure at 330 Ma or the Pangea formation (i.e., ∼80 Myr after the model starts) that differs significantly from the present-day degree-2 structure (Figure 7a) and has significant power at degrees 2, 3, and 4 (Figure 5e). After the Pangea formation, the circum-Pangea subduction helps organize the lower mantle structure to be predominantly degree-2 by ∼250 Ma (Figure 7b at ∼180 Ma and Figure 5e). The lower mantle structure and its time evolution in Case 5 are quite similar to that in Case 3 for the last 200 Ma (Figures 5c, 5e, 6a, 6b, 7b, and 7c). This suggests that the lower mantle structure and its time-dependence for the last 200 Ma in Cases 3 and 5 are insensitive to the mantle structure in the Paleozoic (i.e., no memory of the mantle structure in the Paleozoic).

Case 6 using the Z2010 plate motion results in a cold CMB region in the African hemisphere and a strong degree-1 structure in the lower mantle at 330 Ma (Figures 5f and 7d), due to significant plate convergence between Laurussia and Gondwana before their collision at 330 Ma to form Pangea [*Scotese*, 2001; *Zhang et al.*, 2010]. This result is similar to that from *Zhang et al.* [2010], and the difference is caused by the lack of "ramp-up" time period in Case 6. The circum-Pangea subduction and plate motions after 330 Ma organize the lower mantle structure into degree-2 structure, as discussed before (Figures 5f, 7e, and 7f). By ∼100 Ma, the lower mantle structure in Case 6 (Figure 7f) is quite similar to the present-day degree-2 structure with the African and Pacific thermochemical piles. Notice that in Case 4 that starts at 250 Ma (i.e., the mantle does not have any structure at 250 Ma), the degree-2 lower mantle structure is largely established at 200 Ma and has not changed significantly for the last 200 Ma (Figures 5d and 6d–6f). However, for Case 6, because the lower mantle structure shortly after Pangea assembly differs significantly from the present-day structure, it takes a long time to reach the present-day degree-2 structure. For example, at ∼180 Ma, the CMB region beneath much of Africa (Figure 7e) remains relatively cold and differs noticeably from that at ∼100 Ma (Figure 7f) and the present-day.

3.2. Effects of Mantle Viscosity and Initial Structure

Cases 1–4 with no initial mantle structure showed that the degree-2 mantle structures would develop rather rapidly (i.e., within 50 Myr from the start of model calculations) using either of these plate motion models. This time scale is much shorter than ∼250 Myr that *Bull et al.* [2014] inferred for developing the degree-2 mantle structure. It is interesting to examine to what extent a more viscous lower mantle would slow down the development of the lower mantle structure in response to the surface plate motion. To examine this possibility, Cases 7 and 8 are computed with a reduced Rayleigh number of 7×10^7 and 2×10^7, respectively (Table 2). In Cases 7 and 8, buoyancy number B is also increased slightly to 0.6 and 0.7, respectively, to reduce the entrainment due to the reduced Ra [e.g., *Tackley*, 1998]. However, these cases are otherwise identical to Case 3 including that the models start at 250 Ma. With the reduced Ra, the lower mantle
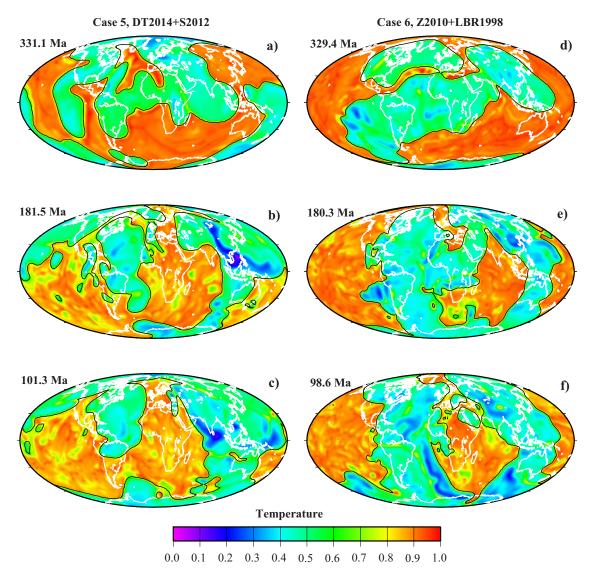
Figure 7. Snapshots of nondimensional temperature at 2750 km depth for Cases 5 and 6 that start at 410 and 458 Ma, respectively. For Case 5 with S2012/DT2014 at (a) ∼330 Ma, (b) ∼180 Ma, and (c) ∼100 Ma, and for Case 4 with LBR1998/Z2010 at (d) ∼330 Ma, (e) ∼180 Ma, and (f) ∼100 Ma. The black contour is for composition field C = 0.5.

viscosity becomes ∼3 × 10²² and 10²³ Pas in Cases 7 and 8, respectively, and the latter is significantly larger than inferred from observations [e.g., *Simons and Hager*, 1997; *Mitrovica and Forte*, 2004].

Cases 3, 7, and 8 show that it takes a longer time to develop similar degree-2 lower mantle structure for models with higher mantle viscosity, as seen in time-dependence of degree-2 power for these three cases (Figure 5g). It takes approximately 30, 70, and 120 Myr for the degree-2 power to reach to 50% of its present-day values for Cases 3, 7, and 8, respectively (Figure 5g). Note that the present-day lower mantle structure is quite similar among these three cases (Figures 6c, 8c, and 8f), although the amplitudes of degree-2 power for the present-day differ by ∼15% (Figure 5g). At ∼180 Ma or 70 Myr after the model calculation starts, Case 3 with the smallest (also most realistic) lower mantle viscosity has a fully developed degree-2 structure in the lower mantle (Figure 6a), but Case 8 with the largest lower mantle viscosity does not have any significant structure yet in the lower mantle (Figure 8d). At this time in Case 7, the degree-2 lower mantle structure just starts to take its form (Figure 8a) with its power reaching to ∼50% of that of the present-day's (Figure 5g). The lower mantle structure at ∼120 Ma in Case 8 (Figure 8e) is similar to that at ∼180 Ma in Case 7 (Figure 8a), showing significant degree-2 structure that is similar to the present-day.
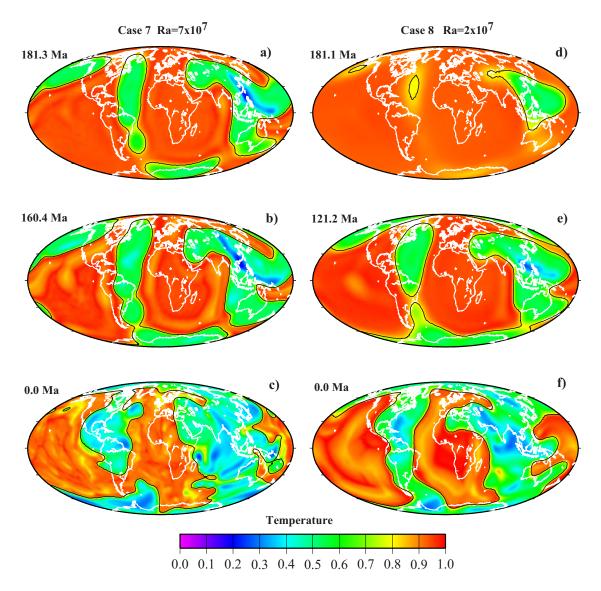
Figure 8. Snapshots of nondimensional temperature at 2750 km depth for Cases 7 and 8 that use different mantle viscosity or Rayleigh number. Both cases start at 250 Ma using S2012/DT2014 plate motion. For Case 7 with Ra = 7 × 10^7 at (a) ~180 Ma, (b) ~160 Ma, and (c) the present-day, and for Case 8 Ra = 2 × 10^7 at (d) ~180 Ma, (e) ~120 Ma, and (f) the present-day. The black contour is for composition field C = 0.5.

Bull et al. [2014] also concluded that using DT2014 and S2012 plate motions for the last 410 Ma, an initially degree-2 mantle structure with African and Pacific LLSVPs (i.e., chemical piles) that is similar to the present-day's mantle would remain unchanged for the last 410 Ma. However, *Bull et al.* [2014] only presented the modeled present-day mantle structure without showing any temporal evolution of thermochemical structure. Case 9 uses an initially degree-2 mantle structure with African and Pacific LLSVPs, but is otherwise identical to Case 5 (i.e., using DT2014 and S2012 plate motions for the last 410 Ma) (Table 2). The initial largely degree-2 temperature and composition fields for Case 9 are taken from the present-day structure for Case 5 (i.e., Figure 9a) and are also nearly identical to the present-day structure for Case 3 (Figure 6c). The mantle structure for Case 9 shows significant temporal evolution in the Paleozoic and early Mesozoic (Figures 5h and 9b). Particularly, the mantle structure in the Paleozoic around 300 Ma (Figure 9b) differs dramatically from the initial degree-2 structure (Figure 9a). Between 350 and 150 Ma, the degree-1 structure is even stronger than the degree-2, although the initial structure is largely degree-2 (Figure 5h). The plate motions before the Pangea assembly in DT2014 are responsible for reducing the degree-2 structure and developing the other structures, similar to those in Cases 5 and 6 and also to *Zhang et al.* [2010]. Plate
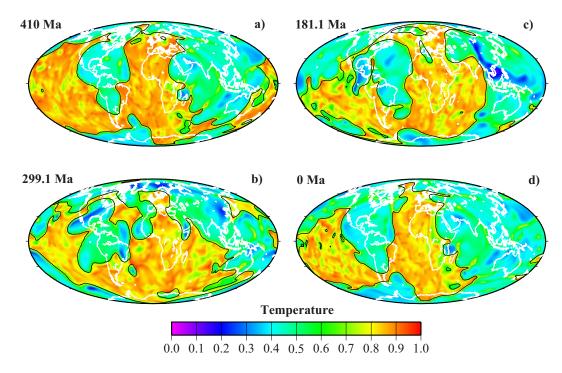
Figure 9. Snapshots of nondimensional temperature at 2750 km depth for Case 9 that starts at 410 Ma using S2012/DT2014 plate motion. Snapshots at (a) 410 Ma or initial condition, (b) ~300 Ma, (c) ~181 Ma, and (d) the present-day. The black contour is for composition field C = 0.5. Note that the initial temperature and composition structure for Case 9 in Figure 9a is taken from the present-day structure for Case 5 and is nearly identical to the present-day structure for Case 9 in Figure 9d after 410 Myr time integration.

motions after the Pangea assembly (i.e., after ~300 Ma) reorganize mantle structures back to their degree-2 form with two thermochemical piles. By ~180 Ma, the thermochemical structures in Case 9 (Figure 9c) become similar to that in Cases 3 (Figure 6a) and 5 (Figure 7b) that start the model calculations at 250 Ma and have different initial conditions, respectively. The subsequent evolution of the lower mantle structure for Case 9 is similar to those for Cases 3 and 5. The present-day structure in Case 9 (Figure 9d) is similar to that in Cases 5 (Figure 9a, i.e., the initial conditions for Case 9) and 3 (Figure 6c).

Case 10 is identical to Case 9, except for using the present-day temperature and composition structure from Case 4 (i.e., Figure 6f) as the initial conditions. The temporal evolution of the mantle structure from Case 10 is similar to that of Case 9. That is, the initially largely degree-2 structure with two thermochemical piles (Figure 6f) becomes largely degree-1 structure in Paleozoic between 350 Ma and 250 Ma. The mantle structure for the last 180 Ma including that for the present-day is nearly identical to that for Cases 9 and 5 that use the same plate motion history model (i.e., DT2014 and S2012).

Cases 11 and 12 differ from Case 9 in having a higher mantle viscosity or smaller Ra (i.e., Ra is 7×10^7 and 2×10^7 for Cases 11 and 12, respectively) (Table 2). However, similar to Case 9, Cases 11 and 12 are computed for the last 410 Ma using DT2014 and S2012 plate motions and initially degree-2 structures that are the present-day structures from Cases 7 and 8, respectively (Figures 8c and 8f or supporting information Figures S1a and S1d). These two cases are designed to examine the possibility that a higher mantle viscosity may help preserve better the initially degree-2 lower mantle structures with two LLSVPs. For both cases, degree-1 and 2 structures in the lower mantle show significant time-dependence that is similar to that from Case 9 (Figure 5h and supporting information Figure S1). That is, for Cases 9, 11, and 12, the first phase of time-dependence is the weakening of degree-2 structure and growth of degree-1 structure (Figure 5h). However, the higher the mantle viscosity is, the slower the change in the mantle structure is. For Case 12 with the largest mantle viscosity, the degree-1 structure is significantly stronger than degree-2 in the lower mantle at the present-day, and it still increases with time (Figure 5h).

Therefore, Cases 9–12 demonstrate that plate motion history model of DT2014/S2012 does not lead to stationary degree-2 mantle structure with the African and Pacific LLSVP piles for the last 410 Ma even if the

mantle structure is degree-2 at 410 Ma and the lower mantle viscosity is as high as 10^{23} Pas. This is in conflict with what *Bull et al.* [2014] have concluded.

4. Discussion

The main objective of this study is to investigate the effects of plate motion history models and mantle viscosity (i.e., Ra) on the temporal evolution of the lower mantle structure since the early Paleozoic in 3-D spherical thermochemical mantle convection models. Our standard models use a mantle viscosity structure that is consistent with inferred from postglacial rebound and geoid modeling (i.e., the lower mantle viscosity of $\sim 10^{22}$ Pas and ~ 100 times weaker upper mantle). For convection models with no initial structure, it takes about ~ 50 Myr to develop dominantly degree-2 structure in the lower mantle with the African and Pacific LLSVPs using the published plate motion history models for the last either 120 Ma [*Seton et al.*, 2012; *Lithgow-Bertelloni and Richards*, 1998] or 250 Ma [*Zhang et al.*, 2010; *Seton et al.*, 2012; *Domeier and Torsvik*, 2014]. The degree-2 mantle structure with two LLSVPs, once formed, shows no significant time-dependence with time till the present-day for either of these plate motion history models.

While the circum-Pangea subduction in plate motion history models between 330 Ma and 180 Ma promotes the formation of degree-2 mantle structure including the two LLSVPs [*Zhang et al.*, 2010], the pre-Pangea plate motion before 330 Ma in the African hemisphere that leads to convergence and collision of continental plates and eventual formation of Pangea, as in both *Domeier and Torsvik* [2014] and *Zhang et al.* [2010] plate motion models, generates nondegree-2 mantle structure. The pre-Pangea plate motion in either of these two plate motion models causes relatively cold lower mantle in the African hemisphere and significant degree-1 mantle structure in the early Pangea (~ 300 Ma). The mantle from the convection model with *Zhang et al.* [2010] plate motion has a stronger degree-1 component than that with *Domeier and Torsvik* [2014], because the former model includes a stronger plate convergence between Gondwana and Laurussia [*Scotese*, 2001] than the latter. The relatively cold lower mantle in the African hemisphere and dominantly degree-1 structure occur at ~ 300 Ma in convection models using the plate motion history by *Domeier and Torsvik* [2014] even when the model starts with the largely degree-2 structure and two LLSVPs as initial conditions at 410 Ma. That is, the African and Pacific LLSVPs cannot be stationary for the last 410 Ma with the plate motion of *Domeier and Torsvik* [2014], in conflict with conclusions in *Bull et al.* [2014].

The circum-Pangea subduction plate motion between 330 Ma and 180 Ma changes the nondegree-2 mantle structure into dominantly degree-2 structure with the African and Pacific LLSVPs generally by ~ 220 Ma for models with the plate motion by *Domeier and Torsvik* [2014] or by ~ 180 Ma for models with the plate motion by *Zhang et al.* [2010]. The difference in timing between these models results mainly from the difference in the lower mantle structure in the early Pangea. The lower mantle has a stronger degree-1 component with colder African hemisphere in convection models with *Zhang et al.* [2010] plate motion than that using *Domeier and Torsvik* [2014] plate motion. Therefore, it takes longer time for models using *Zhang et al.* [2010] to reach the dominantly degree-2 structure. However, the general characteristics of long-wavelength mantle structure evolution as predicted by using these two plate motion models are rather similar. Collectively, these models using either plate motion history models suggest that the present-day mantle structure may have largely been formed by 180 Ma or as early as 220 Ma, and that in the early Pangea and pre-Pangea times, the lower mantle structure may have been very different from the present-day, being relatively cold in the African hemisphere and dominantly degree-1. These results are generally consistent with *Zhang et al.* [2010], but are in conflict with the proposed stationary lower mantle structure with the African and Pacific LLSVPs since the early Paleozoic by *Torsvik et al.* [2010, 2014] and *Bull et al.* [2014].

Higher mantle viscosity would lead to longer response time in developing mantle structure. When the lower mantle viscosity is increased from realistic value of 10^{22} to 10^{23} Pas, the response time in developing degree-2 mantle structure may increase by a factor of 4 from 30 to 120 Myr. While it is unclear what causes the difference between our results and *Bull et al.* [2014], our results with different mantle viscosity suggest that the lower mantle viscosity as high as $\sim 10^{23}$ Pas still cannot preserve degree-2 mantle structures with two LLSVPs for the last 410 Ma for all the plate motion models considered here. Our models also show that it is important to use appropriate mantle viscosity (or Rayleigh number) to study mantle structure evolution.

Now let us address the general question on the mantle structure in the Paleozoic. The mantle dynamic models with the published plate motion history [*Domeier and Torsvik*, 2014; *Zhang et al.*, 2010] strongly

suggest that the mantle in the African hemisphere in the Paleozoic differs significantly from that of the present-day, having significant degree-1 structure and no African LLSVP. However, these results still do not rule out the possibility that the Paleozoic mantle has a largely degree-2 structure that is similar to the present-day's mantle. It is conceivable that a significantly different plate motion history model on the Pangea assembly in the African hemisphere would lead to convergence and subduction patterns that would not significantly perturb the African LLSVP structure in the Paleozoic. For example, in such a plate motion history model, the convergence and subduction responsible for Pangea assembly could occur largely between the two LLSVP upwelling systems and at very different longitudes from those in either *Domeier and Torsvik* [2014] or *Scotese* [2001], and subsequently Pangea would migrate in longitudinal direction relative to the underlying mantle to above the African LLSVP. Admittedly, the latter scenario would be dynamically difficult to achieve, given that Pangea would have to move against the divergent mantle flow from the LLSVP upwelling system. The question is to what extent such a plate motion history model can be constructed robustly and uniquely based on the existing limited geological and geophysical data.

With the extensive analyses on the effects of different plate motions on the lower mantle structure in this study, a relevant question is how the CMB heat flux patterns depend on these different plate motions (e.g., Z2010 or DT2014 plate motions) [e.g., *Zhang and Zhong*, 2011]. Supporting information Figure S2 shows CMB heat flux patterns at three different times for Cases 5 and 6 that are computed for >400 Ma using DT2014 and S2012, and Z2010 plate motion models, respectively. The CMB heat flux is relatively high in regions of the lower mantle with relatively cold temperature [e.g., *Zhang and Zhong*, 2011], although this correspondence may not always hold at relatively small length-scale (supporting information Figure S2). The spectra of CMB heat flux for degrees 1–4 show similar time-dependence to the power of temperature structure in the lower mantle for both Cases 5 and 6 (supporting information Figure S3 and Figure 5). However, the total CMB heat flux for Cases 5 and 6 shows less variability with time except for the initial phase (supporting information Figure S3). The results demonstrate that the lower mantle temperature is a reasonable proxy for long-wavelength CMB heat flux [*Wu et al.*, 2011].

Finally, we would like to point out some potential shortcomings of our models. Our models are no doubt simplified in a number of aspects. We did not attempt to apply any seismic filters to convective structures, as in *Bull et al.* [2009, 2014]. However, since we are mostly interested in degree-1 and degree-2 structures in this work, the filtering effects on mantle structures in our models are likely small. For the convection calculations using DT2014/S2012 plate motion history model for the last 410 Ma, because the plate motion between 250 Ma and 200 Ma is not publically available, interpolated plate motions for this time period used in our models may be different from that in *Bull et al.* [2014]. However, we do not think that the difference would affect our main conclusions, particularly for the mantle structure in the Paleozoic before 250 Ma that should only depend on DT2014 model. We have ignored mantle phase changes such as olivine to spinel, spinel to postspinel, and perovskite to postperovskite. *Zhang et al.* [2010] considered olivine to spinel and spinel to postspinel phase changes, and found only small effects on model results for long-wavelength structure. Considering that the Clapeyron slope of spinel to postspinel phase change, the dynamically more important phase change in the upper mantle, is about -2.5 MPa/K [e.g., *Fukao et al.*, 2009], it is probably a reasonable assumption to ignore upper mantle phase changes in the studies on long-wavelength convection and structure. The perovskite to postperovskite phase change near the CMB would complicate the interpretation of seismic observables from convection models [*Nakagawa et al.*, 2012]. However, its effects on mantle dynamics including the lower mantle structure are rather minor, except for decreasing the stability of the chemically dense piles slightly [e.g., *Li et al.*, 2014] which may be compensated by increasing the compositional density anomalies (i.e., B number) of the piles. We will leave these topics for future studies.

5. Conclusion

We investigated the effects of plate motion history models and mantle viscosity (i.e., Ra) on the temporal evolution of the lower mantle structure since the early Paleozoic by formulating 3-D spherical shell models of thermochemical convection. Our models employ a mantle viscosity structure that is consistent with inferred from postglacial rebound and geoid modeling (i.e., the lower mantle viscosity of $\sim 10^{22}$ Pas and ~ 100 times weaker upper mantle). They also include a layer of chemically distinct and heavy material above the CMB with a volume that is $\sim 2\%$ of the total mantle volume. Our model results can be summarized as follows.

For convection models with realistic mantle viscosity and no initial structure, it takes about ~50 Myr to develop dominantly degree-2 lower mantle structure with African and Pacific LLSVPs that are similar to those in the seismic models, using the published plate motion models for the last either 120 or 250 Ma [*Seton et al.*, 2012; *Lithgow-Bertelloni and Richards*, 1998; *Zhang et al.*, 2010]. However, it takes longer time to develop the mantle structure for more viscous mantle. While the circum-Pangea subduction in plate motion history models promotes the formation of degree-2 mantle structure, the published pre-Pangea plate motions before 330 Ma [*Domeier and Torsvik*, 2014; *Zhang et al.*, 2010] produce relatively cold lower mantle in the African hemisphere and significant degree-1 mantle structure in the early Pangea (~300 Ma), even if the lower mantle initially has a degree-2 structure. This suggests that the African LLSVP may not be stationary since the early Paleozoic. This is also in conflict with a recent mantle convection study by *Bull et al.* [2014] that suggested a stationary degree-2 mantle structure with two LLSVPs for the last 400 Ma, using the plate motion models by *Domeier and Torsvik* [2014] and *Seton et al.* [2012]. With the published plate motion history models, our mantle convection models with realistic lower mantle viscosity (~10^{22} Pas) suggest that the present-day degree-2 mantle structure may have largely been formed by ~200 Ma.

References

Becker, T. W., and L. Boschi (2002), A comparison of tomographic and geodynamic mantle models, *Geochem. Geophys. Geosyst.*, *3*(1), 1003, doi:10.1029/2001GC000168.

Bower, D. J., M. Gurnis, and M. Seton (2012), Lower mantle structure from paleogeographically constrained dynamic Earth models, *Geochem. Geophys. Geosyst.*, *14*, 44–63, doi:10.1029/2012GC004267.

Bull, A. L., A. K. McNamara, and J. Ritsema (2009), Synthetic tomography of plume clusters and thermochemical piles, *Earth Planet. Sci. Lett.*, *278*, 152–162.

Bull, A. L., M. Domeier, and T. H. Torsvik (2014), The effect of plate motion history on the longevity of deep mantle heterogeneities, *Earth Planet. Sci. Lett.*, *401*, 172–182.

Bunge, H.-P., M. A. Richards, C. Lithgow-Bertelloni, J. R. Baumgardner, S. Grand, and B. Romanowicz (1998), Time scales and heterogeneous structure in geodynamic earth models, *Science*, *280*, 91–95.

Bunge, H.-P., M. A. Richards, and J. R. Baumgardner (2002), Mantle-circulation models with sequential data assimilation: Inferring present-day mantle structure from plate-motion histories, *Philos. Trans. R. Soc. London A*, *360*(1800), 2545–2567.

Davies, D. R., S. Goes, J. H. Davies, B. S. A. Schuberth, H.-P. Bunge, and J. Ritsema (2012), Reconciling dynamic and seismic models of Earth's lower mantle: The dominant role of thermal heterogeneity, *Earth Planet. Sci. Lett.*, *353–354*, 253–269.

Domeier, M., and T. H. Torsvik (2014), Plate tectonics in the late Paleozoic, *Geosci. Frontiers*, *5*(3), 303–350.

Dziewonski, A. M. (1984), Mapping the lower mantle: Determination of lateral heterogeneity in P-velocity up to degree and order 6, *J. Geophys. Res.*, *89*, 5929–5952.

Engebretson, D. C., K. Kelley, H. Cashman, and M. R. Richards (1992), 180 million years of subduction, *GSA Today*, *2*, 93–96.

Flowers, R. M., A. K. Ault, S. A. Kelley, N. Zhang, and S. J. Zhong (2012), Epeirogeny or eustasy? Paleozoic-Mesozoic vertical motion of the North American continental interior from thermochronometry and implications for mantle dynamics, *Earth Planet. Sci. Lett.*, *317–318*, 436–445.

Fukao, Y., M. Obayashi, T. Nakakuki, and the Deep Slab Project Group (2009), Stagnant slab: A review, *Annu. Rev. Earth Planet. Sci.*, *37*, 19–46.

Gordon, R. G., and D. M. Jurdy (1986), Cenozoic global plate motions, *J. Geophys. Res.*, *91*, 12,389–12,406.

Grand, S. P., R. D. van der Hilst, and S. Widiyantoro (1997), Global seismic tomography: A snapshot of convection in the Earth, *GSA Today*, *7*(4), 1–7.

Hager, B. H., and R. J. O'Connell (1979), Kinematic models of large-scale flow in the Earth's mantle, *J. Geophys. Res.*, *84*, 1031–1048.

Hager, B. H., and R. J. O'Connell (1981), A simple global model of plate dynamics and mantle convection, *J. Geophys. Res.*, *86*, 4843–4867.

Hager, B. H., R. W. Clayton, M. A. Richards, R. P. Comer, and A. M. Dziewonski (1985), Lower mantle heterogeneity, dynamic topography and the geoid, *Nature*, *313*, 541–545.

He, Y. M., and L. X. Wen (2012), Geographic boundary of the "Pacific Anomaly" and its geometry and transitional structure in the north, *J. Geophys. Res.*, *117*, B09308, doi:10.1029/2012JB009436.

Houser, C., G. Masters, P. Shearer, and G. Laske (2008), Shear and compressional velocity models of the mantle from cluster analysis of long-period waveforms, *Geophys. J. Int.*, *174*(1), 195–212, doi:10.1111/j.1365-246X.2008.03763.x.

Li, Y., F. Deschamps, and P. J. Tackley (2014), Effects of low-viscosity post-perovskite on the stability and structure of primordial reservoirs in the lower mantle, *Geophys. Res. Lett.*, *41*, 7089–7097, doi:10.1002/2014GL061362.

Li, Z. X., and S. J. Zhong (2009), Supercontinent-superplume coupling, true polar wander and plume mobility: Plate dominance in whole-mantle tectonics, *Phys. Earth Planet. Inter.*, *176*, 143–156 doi:10.1016/j.pepi.2009.05.004.

Lithgow-Bertelloni, C., and M. A. Richards (1998), The dynamics of Cenozoic and Mesozoic plate motions, *Rev. Geophys.*, *36*, 27–78.

Masters, G., G. Laske, H. Bolton, and A. M. Dziewonski (2000), The relative behavior of shear velocity, bulk sound speed, and compressional velocity in the mantle: Implications for chemical and thermal structure, in *Earth's Deep Interior: Mineral Physics and Tomography from Atomic to Global Scale*, edited by S. Karato et al., pp. 66–87, AGU, Washington, D. C.

McNamara, A. K., and S. J. Zhong (2004), Thermochemical structures within a spherical mantle: Superplumes or piles?, *J. Geophys. Res.*, *109*, B07402, doi:10.1029/2003JB002847.

McNamara, A. K., and S. J. Zhong (2005), Thermochemical structures beneath Africa and the Pacific Ocean, *Nature*, *437*, 1136–1139.

Mitrovica, J. X., and A. M. Forte (2004), A new inference of mantle viscosity based upon joint inversion of convection and glacial isostatic adjustment data, *Earth Planet. Sci. Lett.*, *225*, 177–189.

Moresi, L. N., and V. S. Solomatov (1995), Numerical investigation of 2D convection with extremely large viscosity variations, *Phys. Fluids*, *7*, 2154–2162.

Moresi, L. N., S. J. Zhong, and M. Gurnis (1996), The accuracy of finite element solutions of Stokes' flow with strongly varying viscosity, *Phys. Earth Planet. Inter.*, *97*, 83–94.

Müller, R. D., M. Sdrolias, C. Gaina, B. Steinberger, and C. Heine (2008), Long-term sea-level fluctuations driven by ocean basin dynamics, *Science*, *319*, 1357–1362.

Nakagawa, T., P. J. Tackley, F. Deschamps, and J. A. D. Connolly (2012), Radial 1-D seismic structures in the deep mantle in mantle convection simulations with self-consistently calculated mineralogy, *Geochem. Geophys. Geosyst.*, *13*, Q11002, doi:10.1029/2012GC004325.

Ni, S., E. Tan, M. Gurnis, and D. V. Helmberger (2002), Sharp sides to the African superplume, *Science*, *296*, 1850–1852.

Olson, P., R. Deguen, L. A. Hinnov, and S. J. Zhong (2013), Controls on geomagnetic reversals and core evolution by mantle convection in the Phanerozoic, *Phys. Earth Planet. Inter.*, *214*, 87–103.

Olson, P., R. Deguen, M. L. Rudolph, and S. J. Zhong (2015), Core evolution driven by mantle global circulation, *Phys. Earth Planet. Inter.*, doi:10.1016/j.pepi.2015.03.002.

Panning, M., and B. Romanowicz (2006), A three dimensional radially anisotropic model of shear velocity in the whole mantle, *Geophys. J. Int.*, *167*, 361–379.

Ritsema, J., H. J. van Heijst, A. Deuss, and J. H. Woodhouse (2011), S40RTS: A degree-40 shear-velocity model for the mantle from new Rayleigh wave dispersion, teleseismic traveltime and normal-mode splitting function measurements, *Geophys. J. Int.*, *184*, 1223–1236.

Rudolph, M. L., and S. J. Zhong (2014), History and dynamics of net rotation of the mantle and lithosphere, *Geochem. Geophys. Geosyst.*, *15*, 3645–3657, doi:10.1002/2014GC005457.

Schuberth, B. S. A., H.-P. Bunge, and J. Ritsema (2009), Tomographic filtering of high-resolution mantle circulation models: Can seismic heterogeneity be explained by temperature alone? *Geochem. Geophys. Geosyst.*, *10*, Q05W03, doi:10.1029/2009GC002401.

Scotese, C. R. (2001), Atlas of Earth history, *Tech. Rep. 90–0497*, Arlington, Tex.

Seton, M., et al. (2012), Global continental and ocean basin reconstructions since 200 Ma, *Earth Sci. Rev.*, *113*(3–4), 212–270.

Simmons, N. A., A. M. Forte, L. Boschi, and S. P. Grand (2010), GyPSuM: A joint tomographic model of mantle density and seismic wave speeds, *J. Geophys. Res.*, *115*, B12310, doi:10.1029/2010JB007631.

Simons, M., and B. H. Hager (1997), Localization of the gravity field and the signature of glacial rebound, *Nature*, *390*, 500–504.

Su, W. J., R. L. Woodward, and A. M. Dziewonski (1994), Degree 12 model of shear velocity heterogeneity in the mantle, *J. Geophys. Res.*, *99*, 6945–6980.

Tackley, P. J. (1998), Three-dimensional simulations of mantle convection with a thermochemical CMB boundary layer: D?, in *The Core-Mantle Boundary Region*, edited by Gurnis et al., pp. 231–253, AGU, Washington, D. C.

Tanimoto, T. (1990), Long-wavelength S-wave velocity structure throughout the mantle, *Geophys. J. Int.*, *100*, 327–336.

Thorne, M., E. J. Garnero, and S. Grand (2004), Geographic correlation between hot spots and deep mantle lateral shear-wave velocity gradients, *Phys. Earth Planet. Inter.*, *146*, 47–63, doi:10.1016/j.pepi.2003.09.026.

Torsvik, T. H., M. A. Smethhurst, K. Burke, and B. Steinberger (2006), Large igneous provinces generated from the margins of the large low-velocity provinces in the deep mantle, *Geophys. J. Int.*, *167*, 1447–1460.

Torsvik, T. H., K. Burke, B. Steinberger, S. J. Webb, and L. D. Ashwal (2010), Diamonds sampled by plumes from the core-mantle boundary, *Nature*, *466*, 352–355.

Torsvik, T. H., R. van der Voo, P. V. Doubrovine, K. Burke, B. Steinberger, L. D. Ashwal, R. Trønnes, S. J. Webb, and A. L. Bull (2014), Deep mantle structure as a reference frame for movements in and on the Earth, *Proc. Natl. Acad. Sci. U. S. A.*, *111*, 8735–8740, doi:10.1073/pnas.1318135111.

Wen, L. X., P. Silver, D. James, and R. Kuehnel (2001), Seismic evidence for a thermo-chemical boundary at the base of the Earth's mantle, *Earth Planet. Sci. Lett.*, *189*, 141–153.

Woodhouse, J. H., and A. M. Dziewonski (1984), Mapping the upper mantle: Three-dimensional modeling of Earth structure by inversion of seismic waveforms, *J. Geophys. Res.*, *89*, 5953–5986.

Wu, B., P. Olson, and P. Driscoll (2011), A statistical boundary layer model for the mantle D-region, *J. Geophys. Res.*, *116*, B12112, doi:10.1029/2011JB008511.

Zhang, N., and S. J. Zhong (2011), Heat fluxes at the Earth's surface and core-mantle boundary since Pangea formation and their implications for the geomagnetic superchrons, *Earth Planet. Sci. Lett.*, *306*(3–4), 205–216.

Zhang, N., S. J. Zhong, W. Leng, and Z.-X. Li (2010), A model for the evolution of the Earth's mantle structure since the Early Paleozoic, *J. Geophys. Res.*, *115*, B06401, doi:10.1029/2009JB006896.

Zhang, N., S. J. Zhong, and R. M. Flowers (2012), Predicting and testing continental motion histories since the Paleozoic, *Earth Planet. Sci. Lett.*, *317–318*, 426–435, doi:10.1016/j.epsl.2011.10.041.

Zhong, S. J., M. T. Zuber, L. Moresi, and M. Gurnis (2000), Role of temperature-dependent viscosity and surface plates in spherical shell models of mantle convection, *J. Geophys. Res.*, *105*, 11,063–11,082.

Zhong, S. J., N. Zhang, Z. X. Li, and J. H. Roberts (2007), Supercontinent cycles, true polar wander, and very long wavelength mantle convection, *Earth Planet. Sci. Lett.*, *261*, 551–564.

Zhong, S. J., A. McNamara, E. Tan, L. Moresi, and M. Gurnis (2008), A benchmark study on mantle convection in a 3-D spherical shell using CitcomS, *Geochem. Geophys. Geosyst.*, *9*, Q10017, doi:10.1029/2008GC002048.